

## **General Disclaimer**

### **One or more of the Following Statements may affect this Document**

- This document has been reproduced from the best copy furnished by the organizational source. It is being released in the interest of making available as much information as possible.
- This document may contain data, which exceeds the sheet parameters. It was furnished in this condition by the organizational source and is the best copy available.
- This document may contain tone-on-tone or color graphs, charts and/or pictures, which have been reproduced in black and white.
- This document is paginated as submitted by the original source.
- Portions of this document are not fully legible due to the historical nature of some of the material. However, it is the best reproduction available from the original submission.

X-692-70-356

PREPRINT

NASA TM X-65345

THE PREDICTION OF CORONAL  
AND  
INTERPLANETARY MAGNETIC FIELDS

K. H. SCHATTEN

SEPTEMBER 1970



GODDARD SPACE FLIGHT CENTER  
GREENBELT, MARYLAND

N70-39765

FACILITY FORM 602

(ACCESSION NUMBER)

(THRU)

(PAGES)

(CODE)

TMX-65345  
(NASA CR OR TMX OR AD NUMBER)

(CATEGORY)



THE PREDICTION OF CORONAL AND INTERPLANETARY  
MAGNETIC FIELDS

K. H. Schatten  
Laboratory for Extraterrestrial Physics  
NASA-Goddard Space Flight Center  
Greenbelt, Maryland 20771

September 1970

---

Invited lecture to be presented at the AIAA Observation and Prediction  
of Solar Activity Conference.

# THE PREDICTION OF CORONAL AND INTERPLANETARY MAGNETIC FIELDS

K. H. Schatten

Laboratory for Extraterrestrial Physics  
NASA-Goddard Space Flight Center  
Greenbelt, Maryland

## Abstract

The advent of high speed digital computers and advances in the understanding of the solar atmosphere have enabled predictions of solar eclipse structure. The magnetic field models, their applications, and limitations are discussed. The effects of solar activity on coronal structure are also discussed. Severny, Wilcox, Scherrer, and Coiburn have recently shown that a high degree of correlation exists between the mean photospheric field and the interplanetary magnetic field. A means for predicting the interplanetary magnetic field is a consequence of their work. An interpretation of this effect is presented that relates to models of the coronal magnetic field.

## I. Introduction

Predictions of solar eclipse occurrences provide us with tests of classical mechanics and information concerning the sun, moon and earth. In a similar manner, recent predictions and observations of solar eclipse structure provide tests of our understanding of astrophysical plasmas and yield new data concerning the behavior of the solar corona.

Early evidence of the importance of the magnetic field in coronal structuring processes was obtained by analogy between the shape of the beautiful polar plumes of the solar corona and the patterns formed by iron filings placed near a bar magnet. Later evidence came with observations of solar magnetism and more recently with the discovery of the solar wind (e.g., Hale;<sup>(1)</sup> Hale and Nicholson;<sup>(2)</sup> Chapman and Ferraro;<sup>(3)</sup> Biermann;<sup>(4)</sup> Chapman;<sup>(5)</sup> Parker;<sup>(6)</sup> and Weber and Davis<sup>(7)</sup>). The presence of a magnetic field embedded within the solar wind that is directly related to the solar magnetic field has been shown by Ness and Wilcox.<sup>(8)</sup>

This leads up to the present day treatment of the interaction of the coronal and interplanetary magnetic field and plasma.

## II. Coronal Magnetic Models

An understanding of the magnetic models of Schatten, Wilcox and Ness<sup>(9)</sup> and Altschuler and Newkirk<sup>(10)</sup> may be aided by referring to Figure 1. This shows the energy density of various components of the solar atmosphere as a function of distance above the photosphere. The data for the figure were obtained by choosing moderate values for the densities, velocities, temperatures and magnetic field strengths within the solar cycle. The energy curves shown are to be interpreted from a somewhat qualitative viewpoint in that uncertainties are likely to be near a factor of 10, and the representation of complex coronal structures by average values is somewhat misleading. Nevertheless, the curves do show the

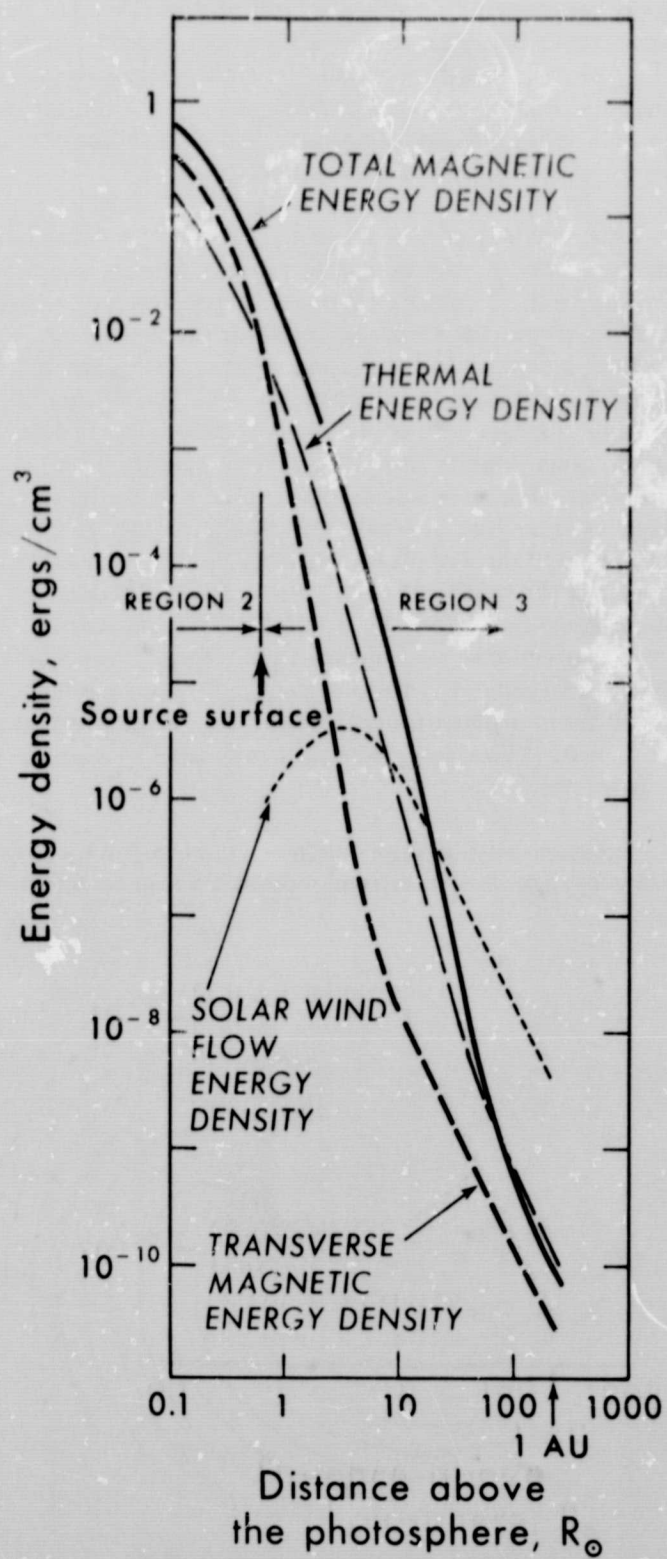


Figure 1. The coronal energy density of the total magnetic field, transverse magnetic field, thermal motion, and solar wind flow versus distance above the photosphere. In region 2 the magnetic field dominates the structure. On the source surface currents flow which allow the field to be transported by the solar wind.

relative importance of various components of the solar corona. Close to the sun, both the magnetic field and the transverse magnetic field predominate, indicating that a force free field configuration results. Beyond about 0.6 solar radii, the coronal plasma thermal energy density supersedes the transverse field energy density. This allows the plasma to stream away from the sun and the field becomes predominantly radial. The Alfvén point is near 20 or 30 solar radii. This is the region where the flow energy density exceeds the field energy density and thus the flow is super-Alfvénic. Escape of the plasma is inevitable beyond this point. Weber and Davis<sup>(7)</sup> give an excellent description of this region.

The topology of the magnetic field in the solar corona as suggested by the magnetic models may be examined in Figure 2. There are three distinct regions in these models where different physical phenomena occur. Region 1 represents the photosphere, where the magnetic field motion is governed by the detailed motions of the plasma near the photosphere. Above the photosphere the plasma density diminishes very rapidly with only moderate decreases in the magnetic energy density. This results in region 2, where the magnetic energy density is greater than the plasma energy density and hence controls the configuration. One may then utilize the force-free condition,  $\mathbf{j} \times \mathbf{B} = 0$ , and in fact make the more restrictive assumption that region 2 is current free. The magnetic field in region 2 may then be derived from a potential that obeys the Laplace equation:  $\nabla^2 \phi = 0$ . The scalar potential may then be employed in this region.

Substantially further out in the corona the total magnetic energy density diminishes to a value less than the

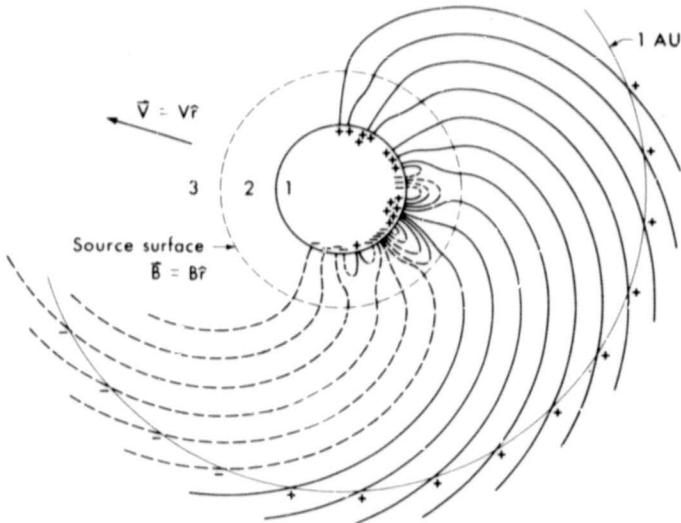


Figure 2. Schematic representation of the source surface model. The photospheric magnetic field is measured in region 1 at Mount Wilson Observatory. Closed field lines (loops) exist in region 2. The field in this region is calculated from potential theory. Currents flowing near the source surface eliminate the transverse components of the magnetic field, and the solar wind extends the source surface magnetic field into interplanetary space. The magnetic field is then observed by spacecraft near 1 AU.

plasma energy density, and the magnetic field can no longer structure the solar wind flow. The magnetic field has, however, become oriented very much in the radial direction, as suggested by Davis.<sup>(11)</sup> Thus, before the total magnetic energy density falls below the plasma energy density, a region is reached where the transverse magnetic energy density does so. It is the transverse magnetic field that interacts with the coronal plasma, since a radial magnetic field would neither affect nor be affected by a radially flowing plasma. Regions 2 and 3 are separated by the surface where the transverse magnetic energy density falls below the plasma energy density. In region 3 transverse magnetic fields are transported by the radially flowing plasma, and can not exist in a quasi-static fashion. The magnetic field existing on the surface boundary between regions 2 and 3 is thus oriented in approximately the radial direction, and serves as a source for the interplanetary magnetic field.

Figure 3 shows this "source surface" superposed upon drawings of coronal eclipse structure from the February 15, 1961 eclipse (by Vsekhsvjatsky,<sup>(12)</sup> top) and the February 25, 1952 eclipse (by Nikolskij,<sup>(13)</sup> bottom). The closed arches fall within the "source surface" sphere. Beyond this distance structures are oriented more nearly radial, in accordance with the model.

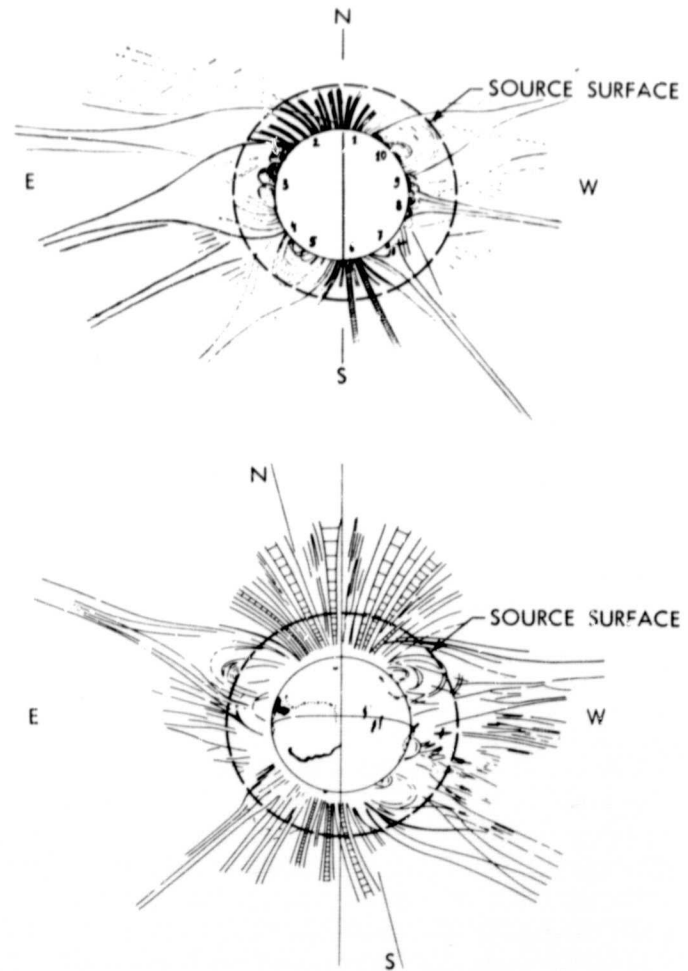


Figure 3. Drawing of the February 15, 1961 eclipse (Vsekhsvjatsky, 1963) (top). Drawing of the corona during the February 25, 1952 eclipse (Nikolskij, 1953) (bottom).

Both the Altschuler and Newkirk and the Schatten, Wilcox and Ness magnetic models are based upon similar physical mechanisms. Only the mathematics in handling the solution and in approximating the observed photospheric magnetic fields differ. Altschuler and Newkirk<sup>(10)</sup> have claimed their technique is superior in its mathematical sophistication. Schatten<sup>(14)</sup> agrees with their mathematical improvements in theory. In practice, however, Schatten<sup>(14)</sup> suggests that uncertainties in the measured photospheric vector magnetic field and in accounting properly for the effects of the coronal plasma outweigh the differences in the two computational techniques.

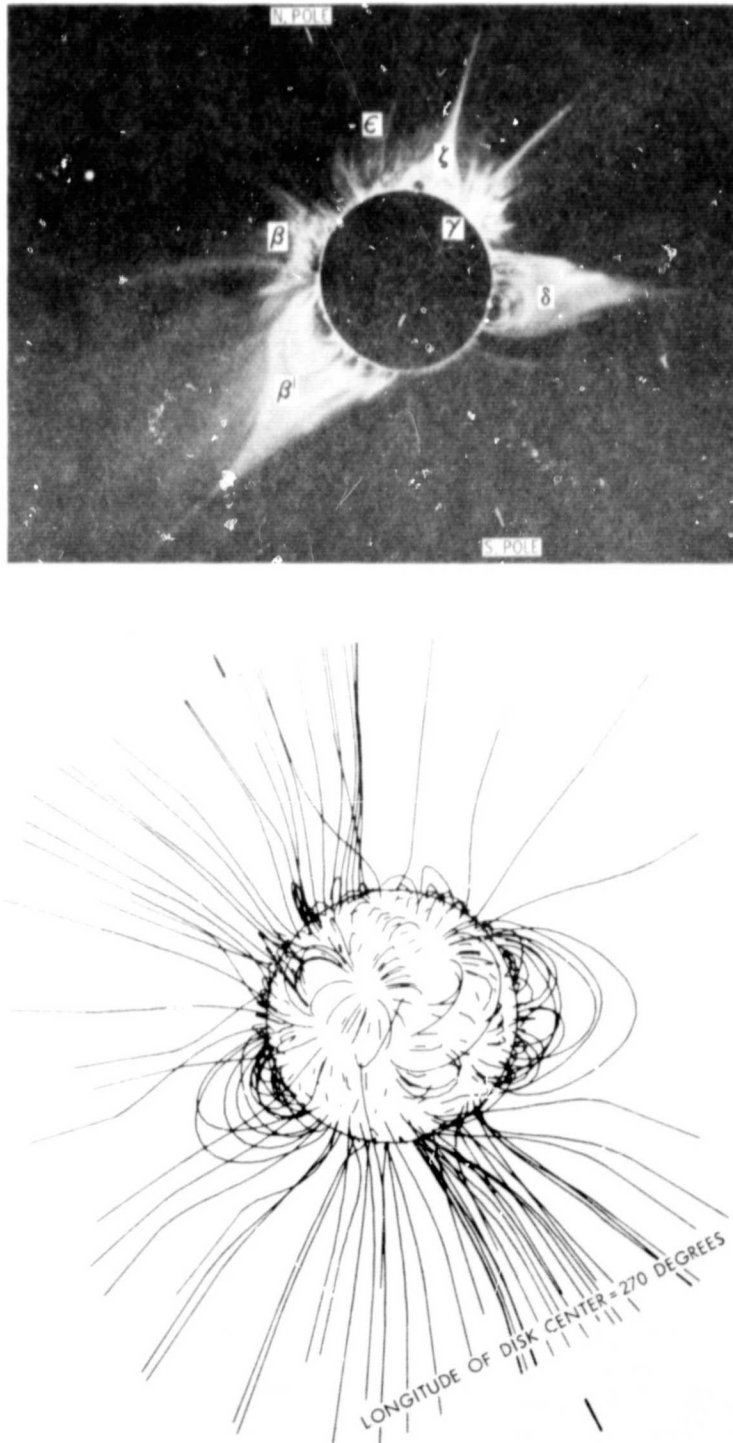


Figure 4. A sketch of the solar corona of November 12, 1966 used to display time scale features (top). Magnetic field line map (bottom) for November 12, 1966 (after Altschuler and Newkirk).

### III. Comparison of Solutions With Eclipse Observations

Comparisons of magnetic field calculations with solar eclipse observations were made for the November 12, 1966 eclipse utilizing both techniques. Figure 4 shows the results of Altschuler and Newkirk<sup>(10)</sup> and Figure 5 that of Schatten.<sup>(15)</sup> Both calculations agree moderately well with each other and with the structure observed in the solar eclipse. It is important to note that there was not very much solar activity prior to this solar eclipse.

The comparisons of computed magnetic fields with observed coronal structure provided encouraging tests of the validity of the models. Other tests were performed as well. The extended coronal magnetic field compared well with the observed interplanetary magnetic field (Schatten, Wilcox and Ness<sup>(9)</sup>). In addition, a Faraday rotation experiment provided information on the coronal magnetic field from 4-12 solar radii that agreed with calculations based on the model of Schatten, Wilcox and Ness (see Stelzried et al.<sup>(16)</sup>).

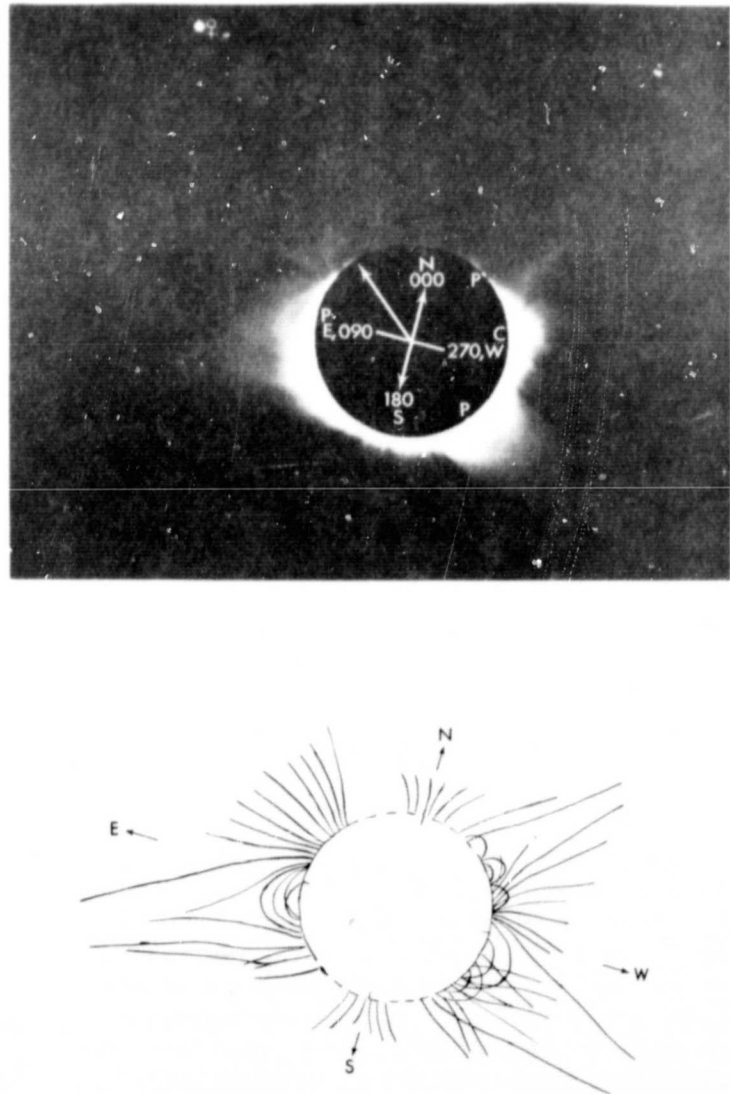


Figure 5. Photograph of the solar corona of November 12, 1966 (top). Sketch of magnetic field line structure for the November 12, 1966 solar eclipse by Schatten (bottom). Note similarity with Figure 4.

#### IV. Prediction of Coronal Structure for September 22, 1968 Solar Eclipse

It then became possible to attempt to predict the structure of the corona at the time of a solar eclipse. Schatten<sup>(15)</sup> did this for the September 22, 1968 eclipse, total over the USSR and western China, and for the March 7, 1970 eclipse, total over Mexico, the US and Canada (Schatten<sup>(14)</sup>).

There are additional difficulties that arise in predicting the structure of the corona at the time of a solar eclipse compared with determining it afterwards. The main problem is with the quality of the photospheric magnetic field data. This information was obtained from the Mount Wilson solar observatory through the courtesy of Dr. Robert Howard. The photospheric magnetic field changes with time due to the appearance of new active centers and the aging of older regions.

If one had perfect observing conditions up to the day of the eclipse, it would be possible to obtain photospheric field information that was about 7 days old on the west limb and 20 days old on the east limb. This is due to the fact that the field is observed near central meridian and the sun rotates from east to west with a period near 27 days as seen from the earth. Near the maximum of the solar cycle the photospheric field can change to some extent within 7 to 20 days. For comparison, there was about one new active region per day forming on the sun during the early part of 1970.

These problems, however, were not the major obstacles encountered in the prediction of the coronal structure for the 1968 solar eclipse. Instead the Mount Wilson magnetograph was experiencing difficulties and it was necessary to make magnetograms from H $\alpha$  photographs and Calcium K2 spectroheliograms of the sun. Utilizing Hale's laws of sunspot polarities together with observations of spot groups, filaments and plage regions it became possible to piece together the magnetic field in the photosphere.

Thus a prediction was made on September 20 concerning the coronal structure of the September 22, 1968 solar eclipse. Figure 6 shows the predicted structure (bottom) and the observed structure (top) by Professor Waldmeier. As can be seen the agreement is quite good. In fact, the comparison between the predicted and actual coronal structure may be better than these two drawings indicate. Koutchmy<sup>(17)</sup> and Pasachoff<sup>(18)</sup> observed small closed arches above the west limb equator that would match those predicted but are missing in Waldmeier's drawing. In addition the arches above the southeast streamer are present in Koutchmy's drawing (Laffineur et al.<sup>(17)</sup>). Cowling<sup>(19)</sup> has stated that the observation "agrees well with the prediction; had Schatten drawn his streamers more nearly radial, the agreement would have been almost perfect."

#### V. Prediction of Coronal Structure for the March 7, 1970 Solar Eclipse

Difficulties were also involved with this eclipse. An inherent difficulty was the high level of solar activity.

SOLAR ECLIPSE  
September 22, 1968

OBSERVATION  
(Waldmeier)

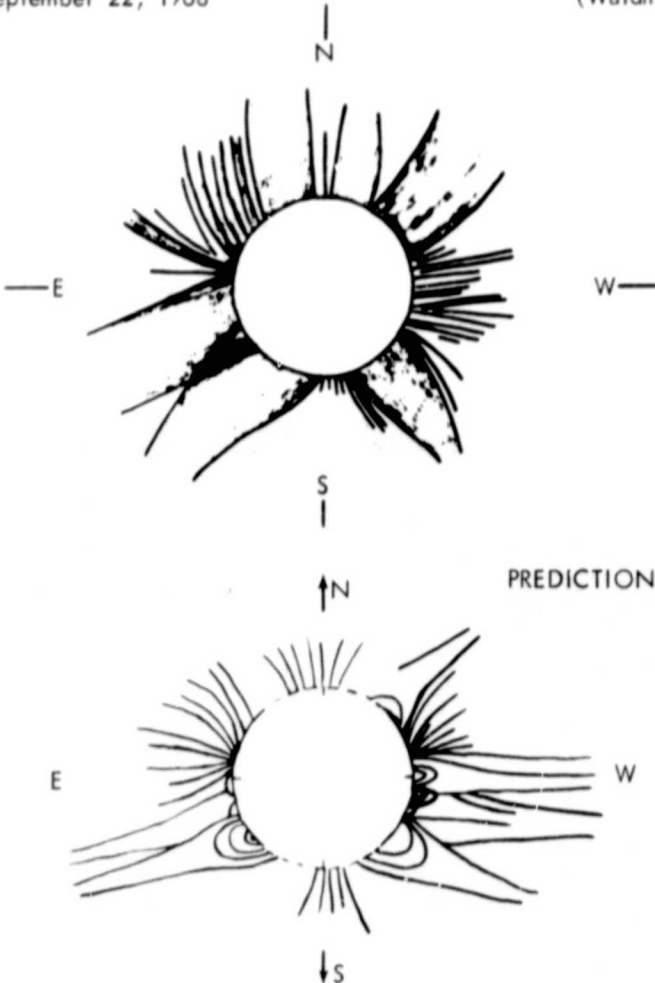


Figure 6. Sketch of the September 22, 1968 solar eclipse drawn by Waldemeier (top). The shaded areas represent streamers. Prediction of the coronal structure drawn on September 20, 1968 (bottom).

Schatten<sup>(15)</sup> pointed out that the magnetic model would not be obeyed in localities of solar flares. In addition, the high level of solar activity would mean that the photospheric magnetic field would be changing more abruptly.

Observations of the photospheric magnetic field were terminated on February 26, 1970 due to poor weather conditions in Pasadena, California. Thus much of the west limb data was close to 34 days old rather than only 7 days old at the time of the eclipse. Figure 7 shows the prediction made by Schatten<sup>(14)</sup> for the coronal structure of the March 7, 1970 solar eclipse.

Figure 8 shows a photograph of the corona at the time of the eclipse taken by Smith (Smith and Schatten<sup>(20)</sup>). Waldemier<sup>(21)</sup> as well as Smith and Schatten<sup>(20)</sup> compared the prediction with observations of coronal structure in the June issue of *Nature* devoted to the eclipse. In both findings comparisons show that there were certain features that agreed well and others that disagreed. Some of the more obvious areas of agreement are the following structures: the long helmet streamer in the NE (position angle 30-70, degrees counterclockwise from the north), short ray open structure in the SW (position angle 210-230), a system of nested arches

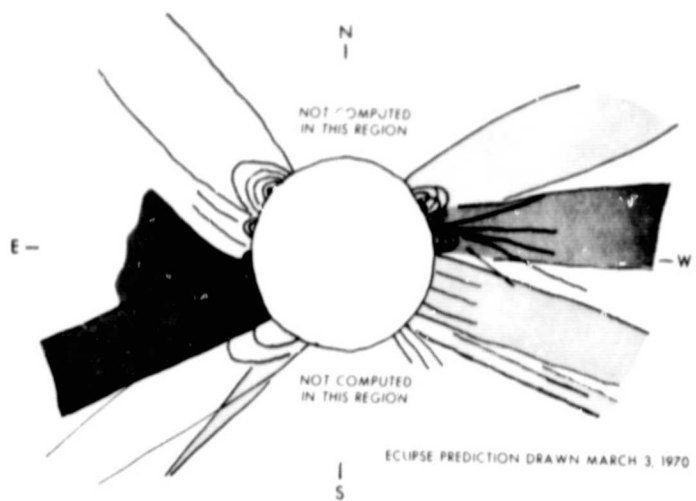


Figure 7. Prediction of the coronal structure for the March 7, 1970 solar eclipse drawn by Schatten. See Figures 8 and 10 for comparison.

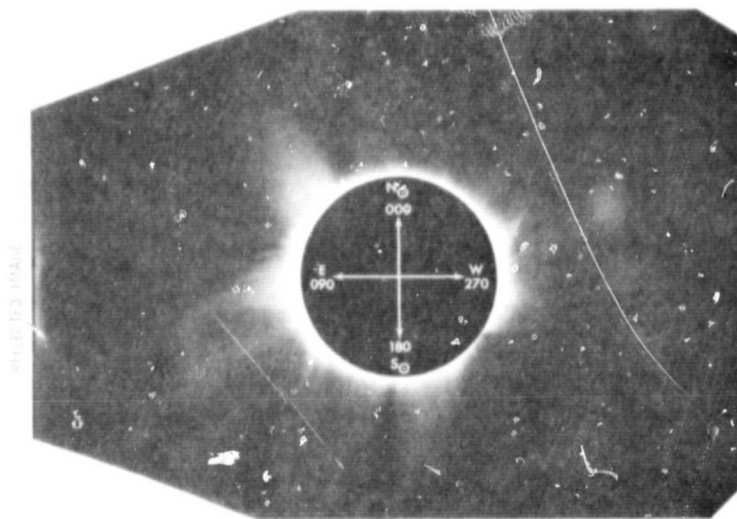


Figure 8. Photograph of the solar eclipse of March 7, 1970 by Smith. Another photograph by Laffineur and Koutchmy is shown in Figure 10 for comparison.

located above the western equator (position angle 292); and a streamer without helmet structure located south of the eastern equator (position angle 100). Waldmeier notes that the region of most serious discrepancy is in the southwest quadrant. The photospheric fields in this region were not well observed prior to the eclipse due to inclement weather at Mt. Wilson. In addition new activity developed there just prior to the eclipse. Martin, Smith and Chapman<sup>(22)</sup> report that on the SW limb an active region began developing on the preceding day around 1700 UT.

Smith and Schatten<sup>(20)</sup> point out that the regions of disagreement are usually associated with coronal condensations. These are located near the equator on the east and west limbs (position angle 109-122, 268-283). These coronal condensations could be a visible manifestation of the flare ejected plasma to be discussed next. The structure of the regions is that of a concave outward series of rays emanating from a small region near

the limb. This is just the shape that would characterize flare ejected field and plasma.

## VI. Flare Ejected Field and Plasma

I would now like to discuss one aspect, perhaps the most significant, of the influence of solar activity upon coronal magnetic field structure. This is the expulsion of magnetic flux from the inner corona by flare activity. The influence of a flare upon the coronal field occurs primarily from the creation of a hotter denser plasma expanding outward from the flare region. We shall therefore discuss the manner in which the coronal magnetic field reacts to this change and the resulting effects upon coronal structure at the time of a solar eclipse.

A unique experiment conducted by Levy et al.<sup>(23)</sup> allowed observations of the coronal magnetic field from 4 to 16 solar radii that enabled an interpretation of this interaction. They measured the Faraday rotation of the microwave signal transmitted by Pioneer 6 as it passed through the solar corona to earth. This Faraday rotation experiment provides a measure of the line integral of the electron density times the component of the magnetic field along the line of sight from the spacecraft to earth. Levy et al.<sup>(23)</sup> report three transient phenomena with Faraday rotations on the order of 40° with a duration of approximately two hours. These Faraday rotation signals were observed when the distances from the sun to the Pioneer 6-earth line of sight were 6, 9 and 11 solar radii.

Schatten<sup>(24)</sup> found evidence for a possible model which produces the Faraday rotation observed by Pioneer 6 while allowing the interplanetary sector pattern to remain intact. This model is shown in Figure 9. A flare of importance 1 or a subflare occurs in the active region

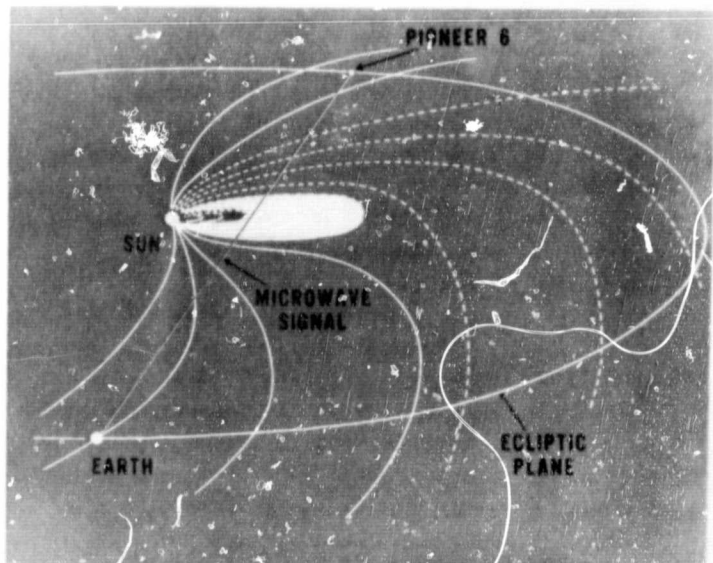


Figure 9. Sketch of the coronal magnetic field line structure as suggested by Schatten from the experiment of Levy et al. The solid lines indicate magnetic field away from the sun and the dashed lines field toward the sun. An enhanced Faraday rotation results when a magnetic bottle is ejected by a flare past the line-of-sight from the spacecraft to earth.

resulting in the heated coronal plasma expanding to produce the magnetic bottle field configuration shown. This field configuration is similar to that proposed by Gold<sup>(25)</sup> for a solar outburst reaching 1 AU. In this case the heated plasma expands the loop coronal magnetic field past the Pioneer 6-earth line of sight at about 10 R<sub>o</sub>. The tension in the magnetic field, however, was shown to be sufficient to prevent the coronal plasma from escaping further into interplanetary space. Thus it appears that even moderate solar activity can influence the coronal structure.

A photo of the corona by Serge Koutchmy is shown in Figure 10 superposed with all the flares and subflares listed in the April, 1970 ESSA bulletin on Solar Geophysical Data that occurred 12 hours prior to the solar eclipse. If the flare ejected plasma emanates radially, the eastern condensation (position angle 109-122) may be explained very well by the activity there. The condensation on the west limb (position angle 268-283) also appears close to active regions recently flaring. In fact it may be the region Martin, Smith and Chapman<sup>(22)</sup> observed. The coronal structure of these regions is that of a series of rays emanating from the location of the flare. The outer portion of the magnetic bottle would lie outside the visible corona and hence would not be seen.

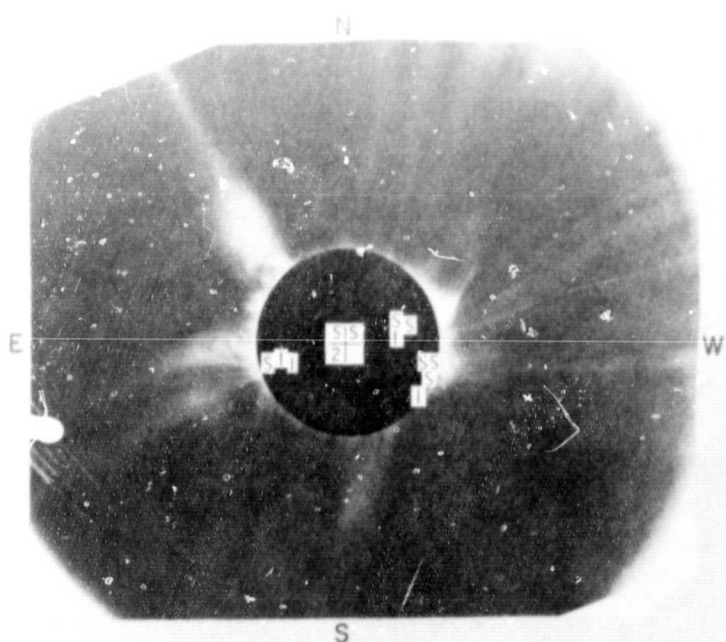


Figure 10. Photograph of the March 7, 1970 solar eclipse by Laffineur and Koutchmy. Superposed are the flares that occurred on the visible side of the sun 12 hours prior to the solar eclipse. The letter "S" indicates a subflare, a 1 indicates an importance 1 flare and a 2 indicates an importance 2 flare.

## VII. Predicting the Interplanetary Magnetic Field

Recently observations of a "mean" solar field (the sun seen as a star) have been made using the Crimean solar telescope (Severny<sup>(26)</sup>). A comparison of the mean solar field with the interplanetary magnetic field was undertaken

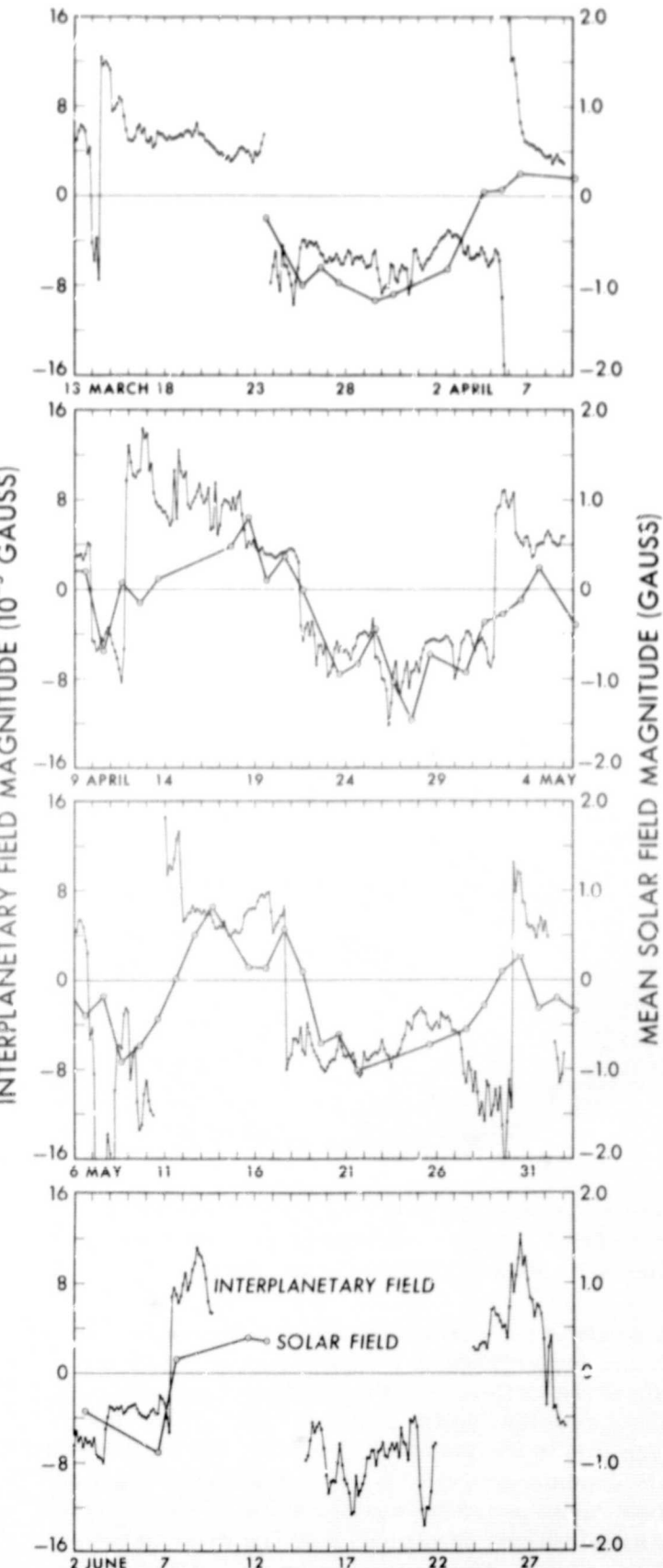


Figure 11. The "mean" solar field compared with the interplanetary magnetic field (after Severny et al.).

by Severny et al.<sup>(27)</sup> Figure 11 shows their comparison. As can be seen, there is good agreement both in sign and magnitude. It is important to note that in the comparison the interplanetary magnetic field is measured 4½ days after the mean solar field to account for transport of the field from the sun to earth.

An interesting effect is that a cross-correlation between the two fields provides a high peak at a lag of 4 $\frac{1}{2}$  days, as expected, but also a larger peak at 27 + 4 $\frac{1}{2}$  days. Schatten et al.<sup>(9)</sup> found this same effect earlier in other work and attribute it to a delay of approximately one solar rotation between the appearance of a new magnetic feature in the photosphere and the resulting change in the interplanetary sector pattern.

Severny et al. note that their work implies that large areas on the sun (mostly outside of active regions) have a field whose predominant polarity agrees with the interplanetary magnetic field polarity. This is an important result in that it implies that most flares do not affect the interplanetary field substantially.

The high correlation that Severny et al.<sup>(27)</sup> have found may allow a prediction of the interplanetary field from mean solar field measurements. By taking the mean solar field in gauss and multiplying by 8, it should be possible to provide an approximate estimate of the interplanetary magnetic field in gammas either 4 $\frac{1}{2}$  days or 31 $\frac{1}{2}$  days in advance.

### VIII. Interpretation of the Mean Solar Field-Interplanetary Field Correlation

Schatten,<sup>(28)</sup> has recently shown that the mean solar field-interplanetary field correlation may be explained from the source surface coronal magnetic model. Figure 12 illustrates the manner in which the source surface model suggests the mean solar field-interplanetary field correlation.

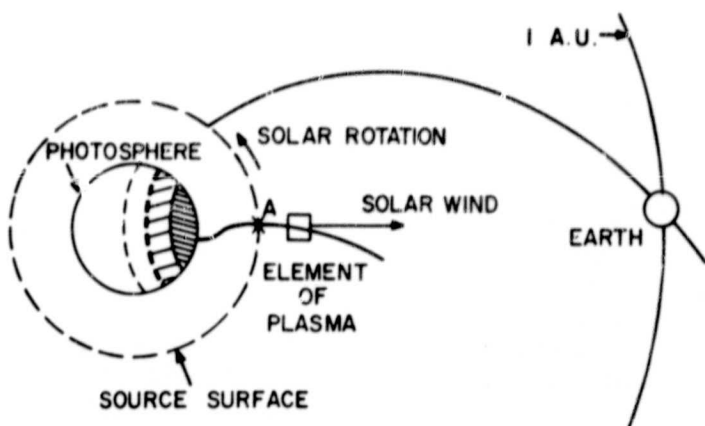


Figure 12. Relationship between the mean solar field, the source surface field, and the interplanetary field. The mean solar field is a weighted average of the disk field (indicated by the shading). The source surface field is the magnetic field on the source surface, position A. This is computed from a weighted average of the photospheric field, quite similar to the mean solar field. The solar wind convects this field to the earth in about 4 $\frac{1}{2}$  days while solar rotation twists the field to approximate an archimedes spiral as shown.

The observed "mean" solar field is an average of the photospheric field over the solar disk with an appropriate weighting factor. This factor is a function of the

angle from a position on the photosphere to the subsolar point. The main contribution to this factor is a result of the difference between the magnetograph measuring the line-of-sight magnetic field and the angular distribution of the photospheric field (perhaps radial on the average). Limb darkening and effects of sunspots, not seen by the magnetograph, are also contributing factors.

The source surface model states that the interplanetary field near the earth results from the source surface field convected by the solar wind outward in about 4 $\frac{1}{2}$  days. Thus the field at the earth is the extended field from position A in Figure 12. The field at position A may be computed in this model as an integral of the photospheric field. This integral also has a weighting factor as a function of angle from the subsolar point and is quite similar to the mean solar field integral. This is seen in Figure 13 where the two weighting factors in

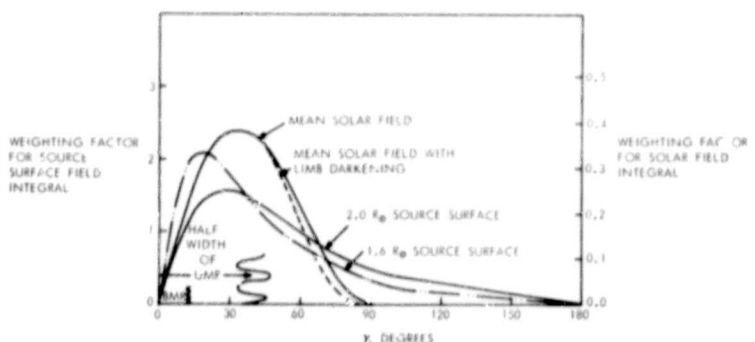


Figure 13. Weighting factor for source surface integrals and mean solar field integral. Note that the shape of the mean solar field weighting factor is very similar to the 2.0 solar radii source surface factor. The half width of a bipolar magnetic region and unipolar magnetic region are shown to indicate the scales over which the photospheric fields are well correlated.

the integrals are shown as a function of angle from the subsolar point. The source surface weighting factors are shown for 1.6 and 2.0 solar radii. Aside from possessing the same shape as a function of angle from the subsolar point, an integration of the weighting factor curves allows the  $8 \times 10^{-5}$  Gauss interplanetary field to 1 Gauss mean photospheric field ratio to be ascertained on theoretical grounds. Thus the agreement between the interplanetary field and the mean photospheric field is viewed as a fortunate coincidence between the source surface weighting factor and the integrated line-of-sight disk factor.

### IX. Magnetic Field Topology in the Solar System During Active Sun Conditions

Evidence will now be presented that suggests the coronal magnetic bottles ejected by small flares are not uncommon. First I shall note a few relevant observations. The interplanetary magnetic field near the ecliptic does not increase in magnitude from solar minimum to solar maximum. The field is roughly 5 gammas

at both times. This indicates that roughly the same number of field lines are leaving the outer corona and extending to 1 AU at solar minimum and at solar maximum. The photospheric field, however, shows great variation between solar minimum and solar maximum. There is a substantial increase in the photospheric field strength at solar maximum. The predominantly open structure of the inner corona from eclipse observations at solar activity maximum indicates much of these additional field lines leave the inner corona; the constant interplanetary field magnitude throughout the solar cycle indicates the additional field lines do not reach 1 AU and in fact do not reach the Alfvén point at 20-30 solar radii as they would then be convected to 1 AU by the solar wind where they are not seen. Thus much of the additional field at solar maximum must reside in magnetic bottles located at 10 to 20 solar radii. Flares are responsible for this field configuration. The field topology of the active solar corona is thus illustrated in Figure 14 in a logarithmic polar coordinate graph.

The central region is the area of greatest interest in this paper. Close to the sun, below about 2 solar radii the corona is stable and inactive coronal magnetic loops may form in accordance with magnetic field calculations. These loops rotate rigidly with the sun. Larger field loops (about 15 solar radii) are ejected by small flares. The inner portion of these loops is in the visible corona and appears as radial rays emanating from a common location. This region is labeled Dynamic as these bottles expand when flare energy is released and contract when cooling. The bottle may extend out to anywhere between 5 and 20 or 30 solar radii. This outer portion of the bottle in general would not be observed by visible

means. Beyond 20 solar radii the field lines are open and form Archimedes spirals which are not shown for clarity. Occasional field loops will emanate from the sun and exist in this region but they will quickly be convected out by the supersonic solar wind. At about 50 AU the field lines presumably merge and the local interstellar field predominates.

## X. Summary and Discussion

Using magnetic models one can calculate the structure of the corona in advance. The method may be tested for accuracy at times of solar eclipses. The method appears to do quite well at times at low activity.

During active times, some of the structures are accurately predicted but other areas are in error. The areas of greatest error are related to active regions and particularly those regions that recently experienced solar flares. The effect of these flares appears in the corona as rays emanating from a common location. It would be possible to predict these, too, by monitoring solar activity up to the time of the solar eclipse. Some errors in these regions would be expected as presumably half the activity would occur on the hemisphere of the sun facing away from the earth and hence could not be monitored. Evidence from spacecraft observations suggest that the field lines emanating from small flares do not extend out to 1 AU but rather return near 15 solar radii.

Recent mean solar field observations and correlations suggest a method of predicting the interplanetary magnetic field in advance. The correlations appear to be consistent and add support to the coronal magnetic models.

## References

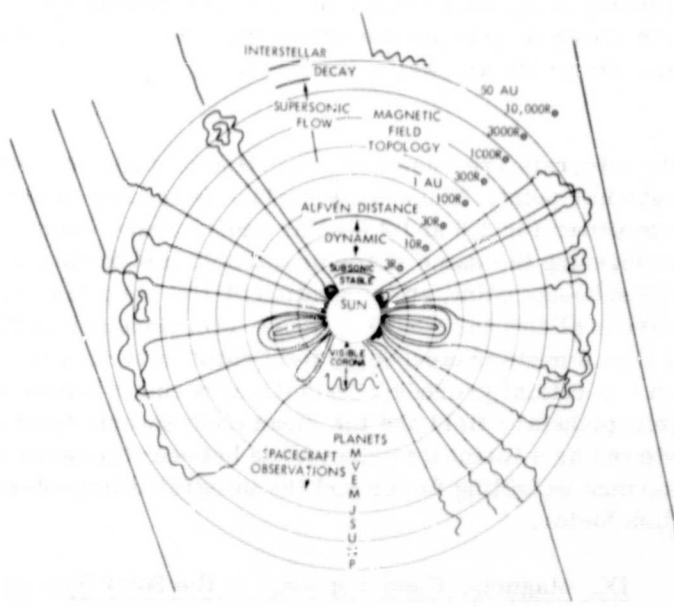


Figure 14. Magnetic field topology in the solar system. Stable loops form above magnetic regions beneath 2 solar radii. Flare ejected loops exist below 20 solar radii. The field is then convected out to the heliospheric boundary at about 50 AU. The spiral and sector structure of the interplanetary field are not shown for clarity.

1. Hale, G. E., Ap. J., 28, 100 and 315 (1908).
2. Hale, G. E. and Nicholson, S. B., Magnetic Observations of Sunspots, 1917-1924 (Washington: Carnegie Institute of Washington, Part 1,) (1938).
3. Chapman, S. and Ferraro, V. C. A., Terrest. Magnetism Atmospheric Electricity, 45, 245 (1940).
4. Biermann, L., Z. Astrophys. 29, 274 (1951).
5. Chapman, S., Smithsonian Contrib. Astrophys. 2, 1 (1957).
6. Parker, E. N., Ap. J. 128, 664 (1958).
7. Weber, E. J. and Davis, L., Jr., Ap. J. 148, 217 (1967).
8. Ness, N. F., and Wilcox, J. M., Phys. Rev. Letters, 13, 461 (1964).
9. Schatten, K. H., Wilcox, J. M. and Ness, N. F., Solar Physics, 6, 442 (1969)
10. Altschuler, M. D., and Newkirk, G., Jr., Solar Physics, 9, 131 (1969).

11. Davis, L., Stellar and Solar Magnetic Fields (ed. by R. Lüst), North-Holland Publ. Co., Amsterdam (1965).
12. Vsekhsvjatsky, S. K. The Solar Corona, (ed. by J. W. Evans), Academic Press, London (1963).
13. Nikolskij, G. M., Astron. Zhurn. 30, 286 (1953).
14. Schatten, K. H., Nature, 226, 251 (1970).
15. Schatten, K. H., Nature, 220, 1211 (1968).
16. Stelzried, C. T., Levy, G. S., Sato, T., Rusch, W. V. T., Ohlson, J. E., Schatten, K. H., and Wilcox, J. M., Solar Physics (1970) to be published.
17. Laffineur., Burnichon, M. -L., and Koutchmy, S., Nature, 222, 461 (1969).
18. Pasachoff, J. (1968) private communication.
19. Cowling, T. G., The Observatory, 89, 217, (1969).
20. Smith, S. M., and Schatten, K. H., Nature, 226, 1130 (1970).
21. Waldmeier, M., Nature, 226, 1131 (1970).
22. Martin, D. C., Smith, S. F., and Chapman, G. A., Nature, 226, 1138 (1970).
23. Levy, G. S., Sato, T., Seidel, B. L., Stelzried, C. T., Ohlson, J. E., and Rusch, W. V. T., Science, 166, 596 (1969).
24. Schatten, K. H., Solar Physics 11, 236 (1970).
25. Gold, T., J. Geophys. Res., 64, 1665 (1959).
26. Severny, A., Nature, 224, 53, (1969).
27. Severny, A., Wilcox, J. M., Scherrer, P. H., and Colburn, D. S., Solar Physics (submitted).
28. Schatten, K. H., Solar Physics (1970) to be published.